XMM OPTICAL MONITOR - TELESCOPE STRAYLIGHT BAFFLE DESIGN AND PERFORMANCE SIMULATION

Document Number XMM-OM/MSSL/TC/0012.01

21 MARCH 1991

Tony Richards, Christina Young

Optical Physics Group
Astrophysics Division
Space Science Department
Rutherford Appleton Laboratory
Chilton,Didcot
Oxon OX11 0QX.

PREFACE

This report describes how a design for the XMM Optical Monitor's straylight baffling system was defined and presents the results of simulating its performance using the GUERAP III program (Generalised Unwanted Energy Rejection Analysis Program).

The results of the study indicate that a minimum Earth-avoidance angle of approximately 25 degrees is likely to have to apply, if straylight levels are to be maintained at or below that equivalent to 1/6 of a mean Zodiacal light level. Also, the study shows that the design of the front of the telescope baffle needs to be refined in order to maintain the required straylight attenuation factor at off-axis angles larger than 60 degrees.

REFERENCES.

'Attenuation Factors for the XMM-OM Baffle', XMM-OM/MSSL/TC/0005.01, 15-Nov-90

TABLE OF CONTENTS

XMM OM BAFFLE DESIGN + PERFORMANCE SIMULATION

1.0 INTRODUCTION - OPTICAL DESIGN DATA.

The XMM Optical Monitor is to be a f/13 Ritchey-Chretien telescope design having an aperture = 155 mm, giving a focal length f = 4030 mm. The back focal length = 249 mm, measured from the primary mirror's surface, on-axis. The particular solution specified for this study for the shapes to be followed by the primary and secondary mirrors are as follows

Primary :	Hyperboloid of revolution, eccentricity of hyperbola	= 1.007714
	conic constant	=-1.015487
Secondary:	Hyperboloid of revolution, eccentricity of hyperbola	= 1.40585
	conic constant	=-1.976413

(N.B. optical design programs normally specify the conic constant K in preference to the eccentricity e, where e**2= - K)

For the purposes of evaluating the straylight performance of the system, it is assumed that a detector having diameter 35 mm is located at the Cassegrain focus of the system (this represents a composite of the so-called 'red'- and 'blue' detectors to be used, the location of the 'blue' detector and the clear aperture required by the focal-reducing optics for the 'red' detector being used). Given the 4030 mm effective focal length, this means that the field of view defined by the detector, which is to be shielded from straylight, subtends an angle of 30 arcminutes on the sky. Thus the FOV semi-diameter is 15 arcminutes, or 1/4 degree.

2.0 PRELIMINARY BAFFLE DESIGN DETAILS.

2.1 BAFFLE LAYOUT AND DIMENSIONS.

Figure 1 shows, to scale, a proposed solution to the problem of baffling the OM telescope system. This is to be regarded as a preliminary design which is to be improved as a result of the present and future studies.

Figure 2 shows the major dimensions, in millimetres, of the preliminary design. The overall length shown for the system puts the front of the telescope tube approximately 7 mm behind its maximum permissable forward position.

2.2 TELESCOPE BAFFLE VANE LOCATIONS.

Figure 3 shows how locations were selected for the baffle vanes required inside the main telescope tube. In the figure, P1 and P2 are diametrically opposite points on the boundary of the primary mirror aperture. B0, B1, Bn etc. are points on the internal edges of the baffle vanes. These latter points are normally located at least 1 degree outside the conical envelope of the clear, unvignetted, circular field of view at the primary, so that light scattered from vane edges towards the primary still has to be scattered through 1 degree before it can enter the FOV of the detector. Since the latter FOV has semi-diameter 1/4 degree, the angle ϕ shown in figure 3 should be 1.25 degree at least. In the present design, it has been chosen to be the minimum, 1.25 degrees.

The position for B0 is where the line leaving P1 at angle ϕ to the optical axis cuts the plane defining the front of the telescope tube. The position for B1 was selected to be where the line from P2 to the point where baffle B0 meets the tube wall cuts the line from P1 to the edge B0 of the front baffle. The positions for baffles B2,B3 and so on, were selected as shown for the baffle pair Bn and Bn+1.

Point 'O' is a point on the edge of the front vane, diametrically opposite point B0. The line from O to Bn cuts the telecope wall at W1. The location of Bn+1 is chosen where the line P2->W2 cuts the line P1->B0 such that the position W2 where the line P2->Bn+1 cuts the telescope wall is a specified amount (in this case 5 mm) FORWARDS of W1. This 5 mm overlap ensures that the region of the wall between 2 baffle vanes which can be seen from a point on the primary mirror CANNOT simultaneously be illuminated DIRECTLY by light entering through the front aperture of the telescope tube.

By having to have ϕ = 1.25 degrees and by locating the front baffle B0 at 1110 mm forward from the edge of the primary mirror, it can be seen that the telescope tube inner radius must be at least 188 mm in order to have a reasonable depth available for baffle vanes, if their number is to be kept to a reasonable value (figure 2 shows that the radius of the aperture in baffle B0 must be at least 179.2 mm). More vanes means more vane edges, which means more edge scatter, so the more depth available for the vanes the better since this means fewer vanes required to shield a given tube length.

The telescope tube wall is shown with a 'step' at about 460 mm forwards of the primary as a concession to possible radial constraints in this area and with a view to mass-saving. However, the 175 mm internal radius shown for the telescope tube between this point and the primary is regarded as a minimum consistent with minimum baffle vane numbers and maximum baffle vane efficiency.

2.3 PRIMARY MIRROR BAFFLE INTERNAL VANES

The baffle vanes shown inside the primary baffle tube (see figure 1) were located in a fashion similar to that used for the main telescope baffle vanes, only this time using points F1 and F2 on the edge of the detector (instead of points P1 and P2) and points on the tip of the conical primary baffle wall (in place of points B0 and O).

2.4 SECONDARY AND PRIMARY MIRROR BAFFLES

Figure 4 shows what constraints act to define the region which can be occupied by the primary and secondary mirror baffles. In that figure, all dashed lines are either the optical axis or define the directions of rays which converge on the point of intersection of the optical axis with the image plane (the axial image point). All continuous lines define rays which, on entering the system through points E1 and E2 on the entrance aperture, converge to diametrically opposite points on the edge of the detector area. These latter rays serve to define the regions occupied by rays which enter the entrance aperture within the angular range defined by the FOV of the detector. In figure 4, the angle α = 1/4 degree, the FOV semi-diameter. The points A and B mark the furthest extents from the secondary and primary mirrors of their respective baffles, if no vignetting of the FOV is to be permitted. Again, if no vignetting is to be permitted, the secondary baffle structure must fit within the volume between the cones of revolution formed by rotating lines E2->A and A->S1 about the optical axis. Similarly, the primary baffle structure must fit within the volume between cones formed by rotating lines P2->B and B->F1 about the optical axis (which is the axis of symmetry for the system).

The driver for the actual shapes and locations of the primary and secondary mirror baffles is the combination of axial and radial location chosen for point E2. The design is most sensitive to the RADIAL location of E2, so it makes sense to specify a reasonable axial location for E2 (in the present case it is located in a plane 51 mm from the secondary mirror surface) and then proceed to an optimum choice for the radial location of E2. Once a location for E2 is fixed, a subsequent location for point Tp, on the extreme forward internal tip of the primary baffle cone, can be selected, bearing in mind the knowledge that the tip of the cone cannot be infinitely sharp. The design is then fixed by ensuring that a value for E2 is selected such that a line from E2->Tp when continued to the image plane MISSES the detector by a preset 'safety margin'. For the baffle design shown in figures 1->4, the latter safety margin was taken = 5 mm. The latter precaution is absolutely essential in order to ensure that no light can directly reach the detector from the space forwards of the extreme outer edge of the secondary baffle.

The present preliminary design uses a radial location for E2 = 56 mm from the telescope axis and an axial location = 700 mm forward from the image plane. The resulting secondary baffle system creates an obstruction having a diameter = 0.36 times the primary aperture (obstruction ratio Q = 0.36). This means a through-put of 100 *(1-Q)(1+Q) = 87 percent of the full-aperture value. Even with no secondary baffle, but with a minimum secondary diameter = 32 mm (obstruction ratio Q= 0.2), the maximum through-put is 100*(1-0.2)*(1+0.2) = 96 percent, so the added secondary baffle changes the through-put by 9 percent.

The shape and size of the baffles depends strongly on the configuration of the mirrors and on the size of the field of view that must be free from vignetting. The present design gives a 30 arcminute diameter unvignetted FOV. Reduction in the diameters of the primary and secondary baffle vanes would result in a loss of off-axis light. Figure 5 shows the appearance of the tips of the primary and secondary baffles as viewed on the entrance pupil plane from the object points, in this case at infinity, showing an unvignetted FOV through the telescope.

2.5 SECONDARY MIRROR SUPPORT STRUTS

Final structural items which turn out to have a critical impact on the straylight scatter at smaller off-axis angles are the 4 equispaced struts chosen to support the secondary from the telescope tube wall. An idealised design was chosen for these. They were envisaged as being equilateral-triangular in cross-section normal to their length, with a triangle-side length = 3 mm. The face making up the base of the triangle is oriented in the telescope so as to face directly towards the primary mirror. The proportion of the cross-section, combined with the struts' location and orientation means that neither of the other two faces of each strut can be seen by the primary mirror, ensuring that light scattered from these surfaces cannot reach the primary directly.

3.0 GUERAP III MODELLING.

The structure shown in figure 1 was broken down into constituent parts modellable using planes , cones, cylinders, hyperboloids, toroids etc. and a 250-surface model of it created as a data set for running the GUERAP III straylight analysis program on it. Figure 6 shows 2 alternative versions used to model the edges of the planar baffle vanes. Each version consists of a hyperbolically-profiled tip with a bevel added to one face. All planar baffle vanes are oriented with the bevel side TOWARDS the incoming light.

The details of the technique used to model and run GUERAP III will not be given here. Suffice it to say that the program produces estimates for the system 'Attenuation factor' which is just the reciprocal of the 'Point Source Transmittance' (PST) as shown in figure 7.

Some details which must be given though, are the optical properties given to the most important surfaces.

All the internal baffle surfaces, including the baffle vane edges, were assumed to be given a black absorbing coating with the following properties:

Absorption coefficient = .995

Diffuse scatter coefficient = 0.005

The primary and secondary mirror surfaces were assumed to have the following properties

Specular Reflectivity = 0.99778

Diffuse Reflectivity = 0.00200

Near-specular scatter fraction = 0.00022

The near-specular component was assumed to obey the following law with angle α from the specular direction (α in radians)

$$S(\alpha) = 0.014 \exp(-20\alpha) \text{ per steradian}$$

This function is plotted in figure 10, together with the diffuse scatter component and their sum total, as a function of angle . Note that the total scatter function = 0.01 at 1 degree from specular. The above numbers indicate the very best achievable for the baffle absorbing coating. The mirror performance figures are what can be expected from a moderately smooth, very clean mirror, the diffuse component being fairly small. The PST at angles from 20 degrees to 80 degrees off-axis was estimated and the results are shown in figure 8. The error bars shown in the figure reflect the statistical uncertainty resulting from the Monte Carlo nature of the GUERAP III analytical approach. Typically 100000 rays were traced from the telescope tube aperture in each run.

4.0 RESULTS AND DISCUSSION.

In figure 8, a horizontal dotted line is drawn at the value of the PST which is required to attenuate the signal from the illuminated Earth, seen from XMM at its nominal altitude, to a level at the detector equivalent to that 1/6 of a mean Zodiacal light background level (see Appendix A for how this figure was derived). A PST value SMALLER than this will ensure a background level SMALLER than the target value, for the same incident intensity.

It can immediately be seen that the baffle system's PST exceeds the required value at off-axis angles smaller than about 25 degrees. Also, it has been found that the required PST is likely to be exceeded at off-axis angles larger than approximately 65 degrees UNLESS the design of the front portion of the telescope containing the first 5 baffle vanes is not modified. In figure 8, the triangles (joined to the rest of the graph by dashed lines) showing results at off-axis angles 70 and 80 degrees were obtained using a baffle edge design shown in figure 6a, whereas the LOWER values of PST at the same angles were obtained using the edge-design shown in figure 6b. The difference that using design 6b makes is that incident light must enter at an angle greater than 80 degrees to the axis before it can illuminate the innermost edge of the vane, from where it can scatter light directly towards the primary mirror. With design 6a the incident angle need only exceed 60 degrees to produce the same scatter route.

Figure 9 allows one to interpret the behaviour of the results shown in figure 8 for angles between 30 and 20 degrees off-axis. At 30 degrees, light entering the front of the telescope tube is only just beginning to illuminate those regions of the telescope wall and those baffle vane surfaces which can scatter light towards the surfaces of the secondary support struts which face the primary mirror. As the angle drops from 30 deg to 25 deg, more and more surfaces are illuminated which scatter light to the secondary strut surfaces, from which light is subsequently scattered directly into the detector's field of view and towards the primary mirror, eventually to reach the detector via specular reflections from both primary and secondary mirror surfaces.

As the angle drops further, regions of the telescope tube wall and baffle vane surfaces are eventually illuminated which can scatter light, not just towards the secondary support struts, but directly towards the secondary mirror surface (and also secondary baffle internal vane surfaces), whence light can be eventually diffusely scattered directly to the detector.

6.0 CONCLUSIONS.

The following are the main conclusions.

- The required PST is achievable for off-axis angles between approximately 25 degrees and 80 degrees.
- Achievement of the required PST at off-axis angles from 80 deg. to 90 deg. will require improvement of the performance of the front section of the telescope tube, possibly involving some increase in diameter in order to create a short first stage section which can shield the entrance aperture of the main telescope tube, from objects more than 80 deg. off-axis.
- The required PST performance will only be achieved using the best absorbing coating available for the baffle walls and vane edges and maintaining scrupulously clean primary and secondary mirror surfaces.

APPENDICES

APPENDIX A. XMM OM POINT SOURCE TRANSMITTANCE REQUIREMENT

In this appendix an estimate is made for the Point Source Transmittance (PST) of the baffled XMM OM system which is required in order to attenuate Earthlight at 45 degrees off-axis to an acceptable level. A reference document from which some data is drawn is XMM-OM/MSSL/TC/0005.01, dated 15-Nov-90.

Figure 7 in the main report defines the PST of the system in terms of irradiances at the front of the system and at the detector. The irradiance Fe at the front of the XMM OM system is to be taken as that of the sunlit Earth viewed at 45 degrees off-axis and at an altitude of 40000 KM (the XMM operating altitude). In the reference document, this irradiance is given in terms of that given by an equivalent number of 10th magnitude G0 stars and is

$$Fe = 3.24 \times 10^{12} \quad (Mv=10, G0 \text{ stars})$$

The dimensions of Fe are energy/unit area/unit time.

The permissable irradiance at the detector is specified in the reference document as equivalent to 1/6-th of a mean Zodiacal light background intensity AT THE DETECTOR. The analysis proceeds as follows -

Let Fz be the mean intensity of Zodiacal light per unit solid angle of sky AT THE TELESCOPE APERTURE. Then (see figure 7) the energy in Zodiacal light collected by the detector is given by

$$Ed = Fz. Ao . d\Omega$$

where Ao = area of telescope aperture = $(\pi/4)$.Do**2 if the central obstruction is ignored for the moment,
and $d\Omega = (\pi/4)$.Ad/f**2 , the solid angle subtended by the detector.

?

The mean irradiance at the detector due to this light, Fd^{z} , will therefore be given by dividing Ed by $(\pi/4)$.Dd**2, the area of the detector, resulting in the following expression for Fd^{z}

$$Fd^{z} = Ed/(\pi/4)/Dd{*}{*}2 = Fz.(\pi/4).(Do/f){*}{*}2$$

f/Do is just the f-number of the telescope (f/Do=13 in the present case). The quantity, Fz, is given in the reference document as equivalent to 81 Mv=10,G0 stars per square degree. If we convert the value for Fz to number of Mv=10 stars per steradian (by dividing it by $(\pi/180)$**2), then the permitted irradiance at the detector becomes Fd where

$$Fd = Fd^{z}/6 = (81/6).(180/\pi){*}{*}2.(\pi/4).(1/13){*}{*}2 = 206 \quad Mv=10, \text{ G0 stars}$$

The required PST for the system then becomes just Fd/Fe which evaluates to

$$PST <= 206/3.24\text{x}10^{12} = 6.36 \times 10^{-11}$$

The equivalent baffle Attenuation factor us just 1/PST = 1.6×10^{10} .

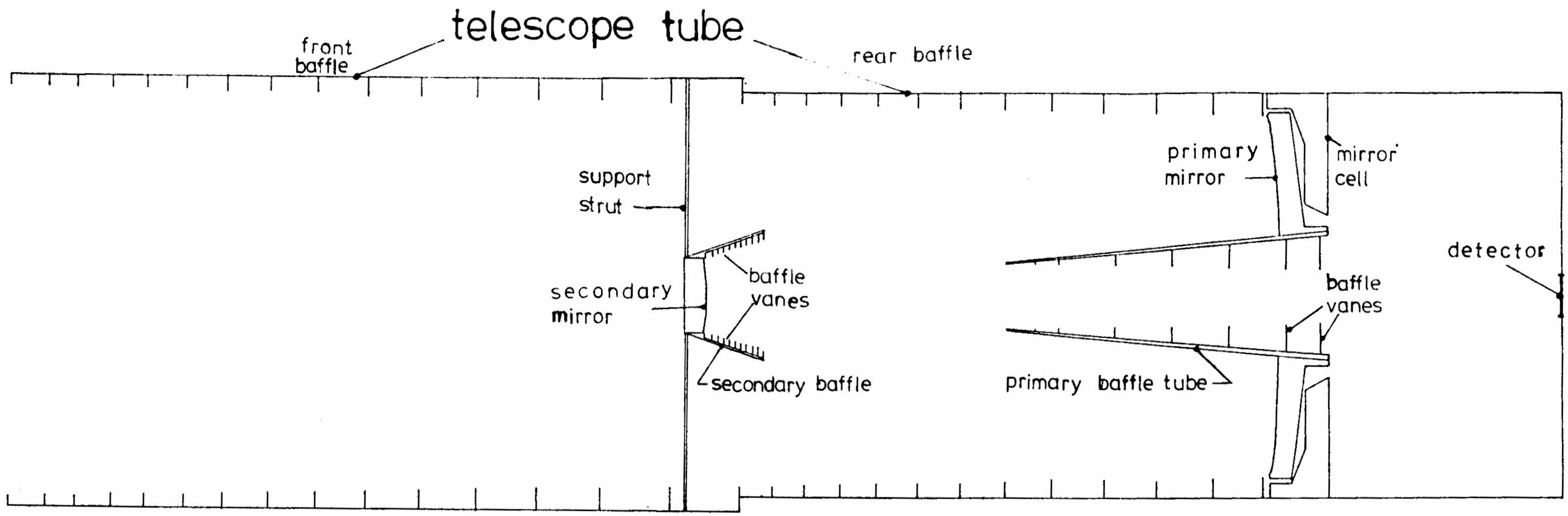

Figure 1. A Proposed XMM Optical Monitor Baffle Design

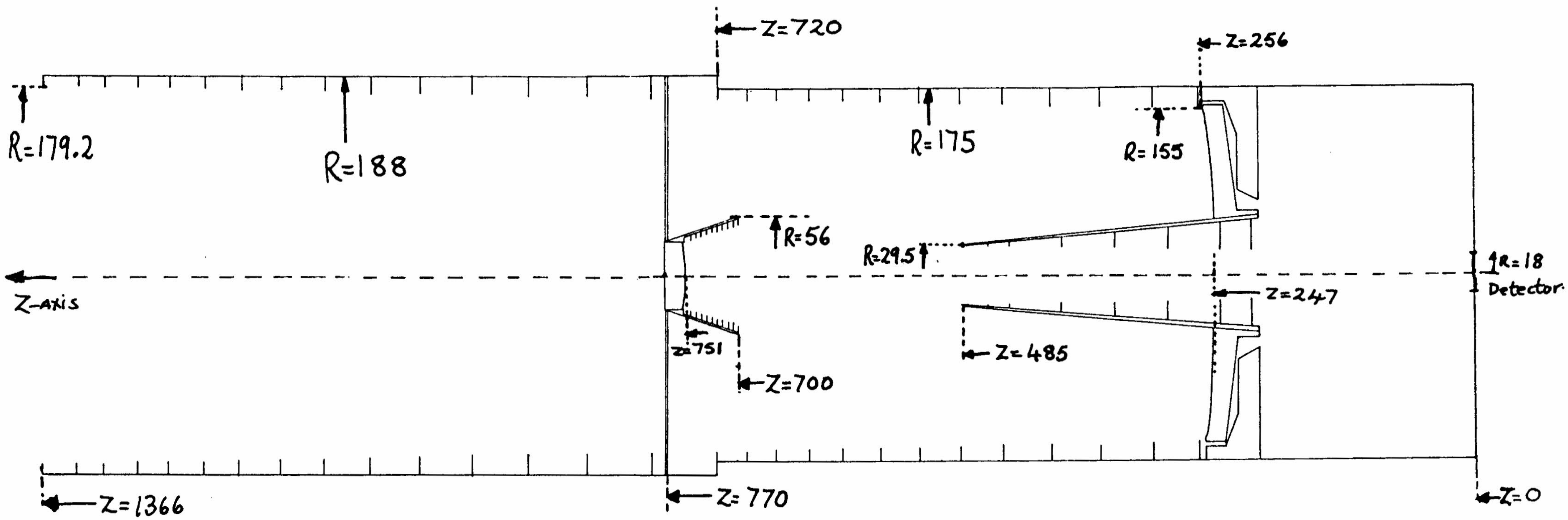

Figure 2. Major Dimensions (in mm) of the Proposed XMM OM Baffles

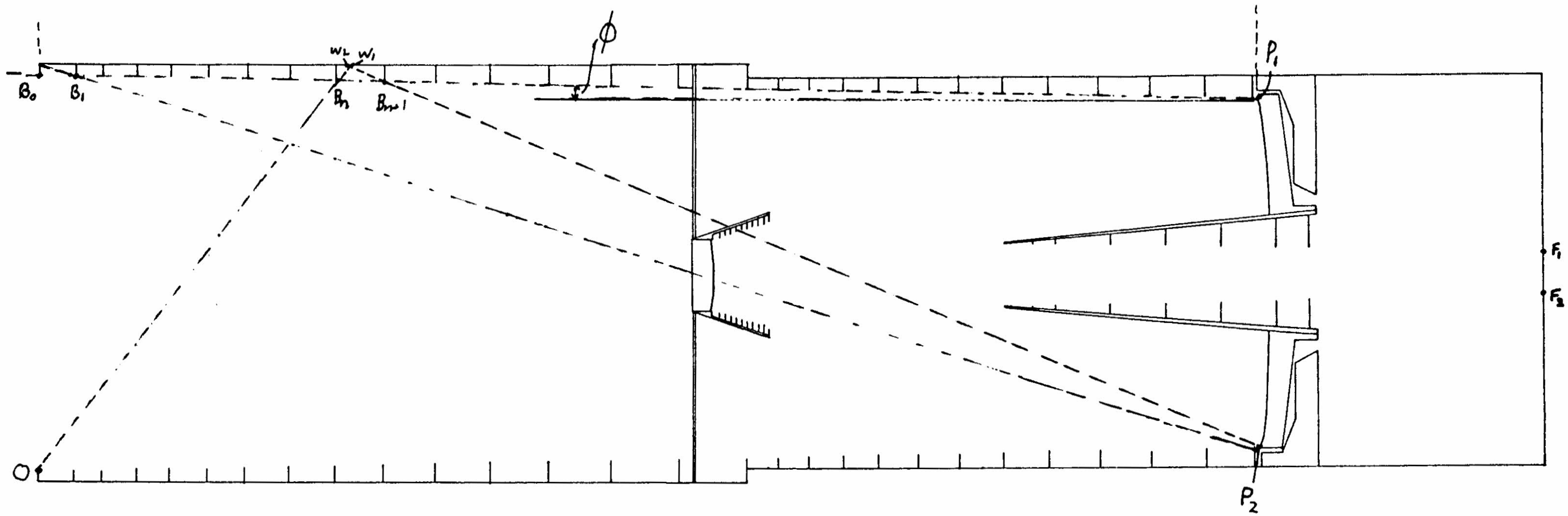

Figure 3. How Telescope Tube Baffle Vane Locations are Defined

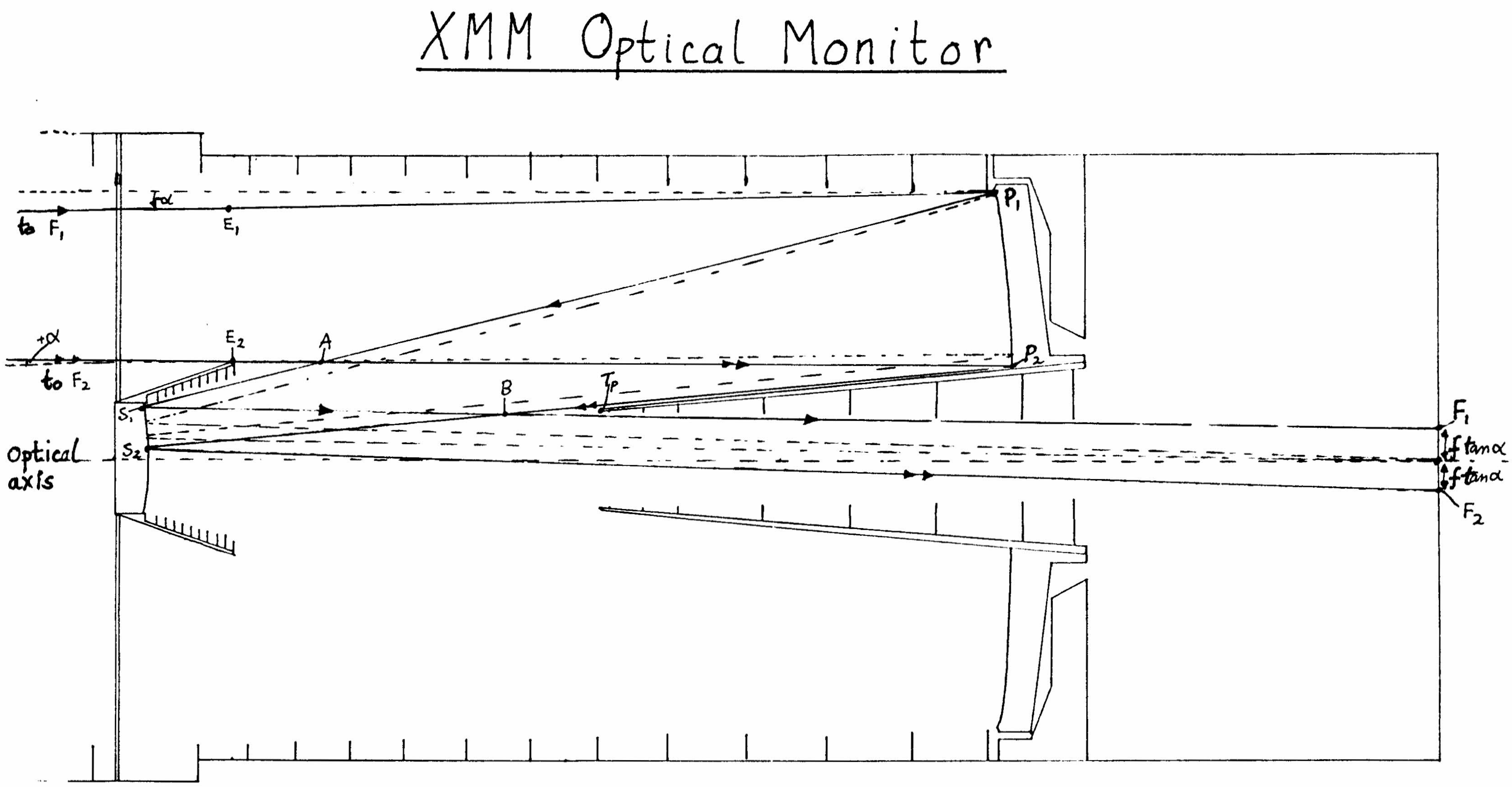

Figure 4. How the Spaces Available for the Primary + Secondary Mirror Baffle Structures are Defined

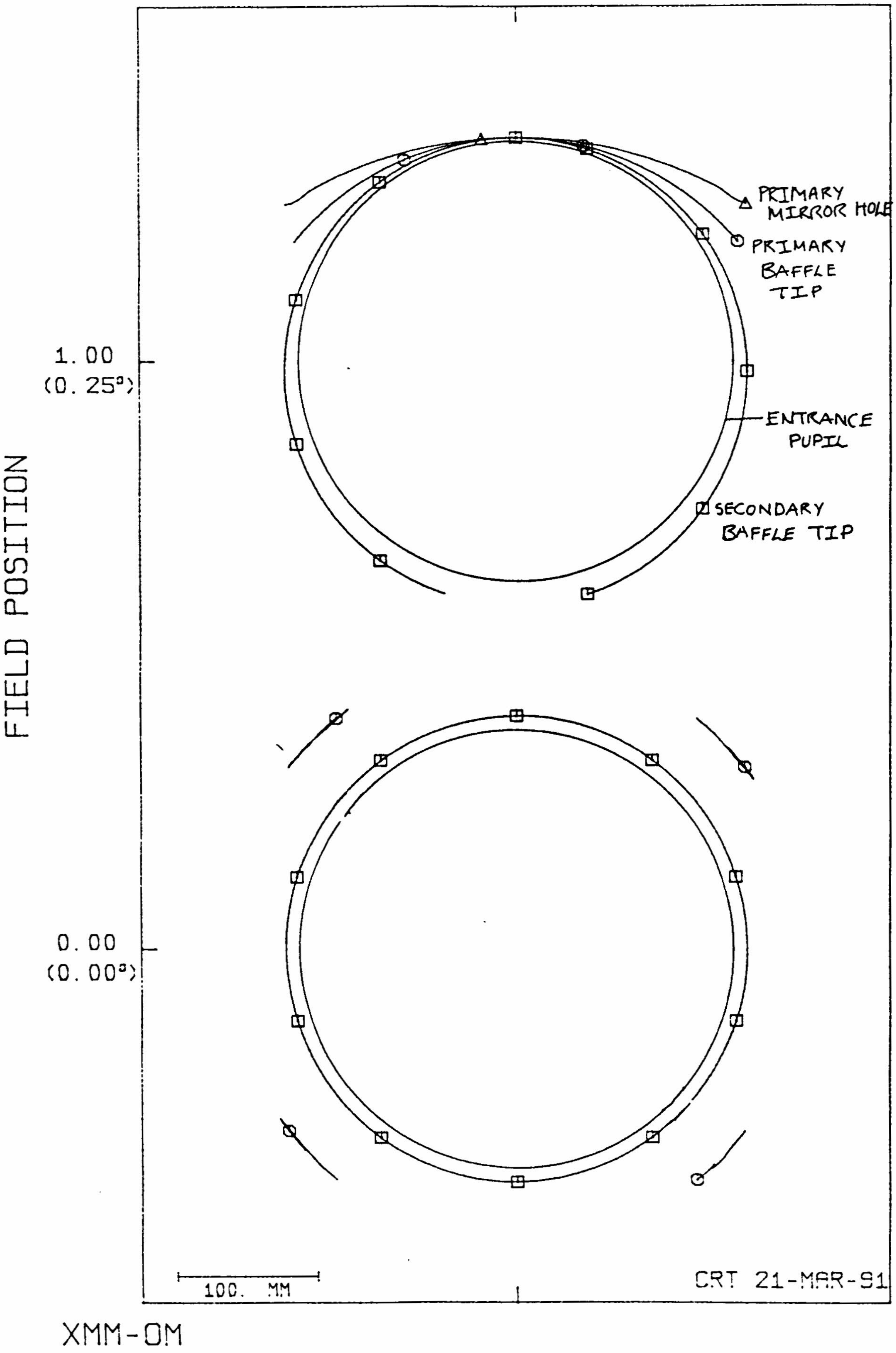
PRIMARY MIRROR HOLE
PRIMARY BAFFLE TIP
ENTRANCE PUPIL
SECONDARY BAFFLE TIP
1.00
(0.25°)
0.00
(0.00°)
FIELD POSITION
100. MM
CRT 21-MAR-91
XMM-OM

FIG. 5.

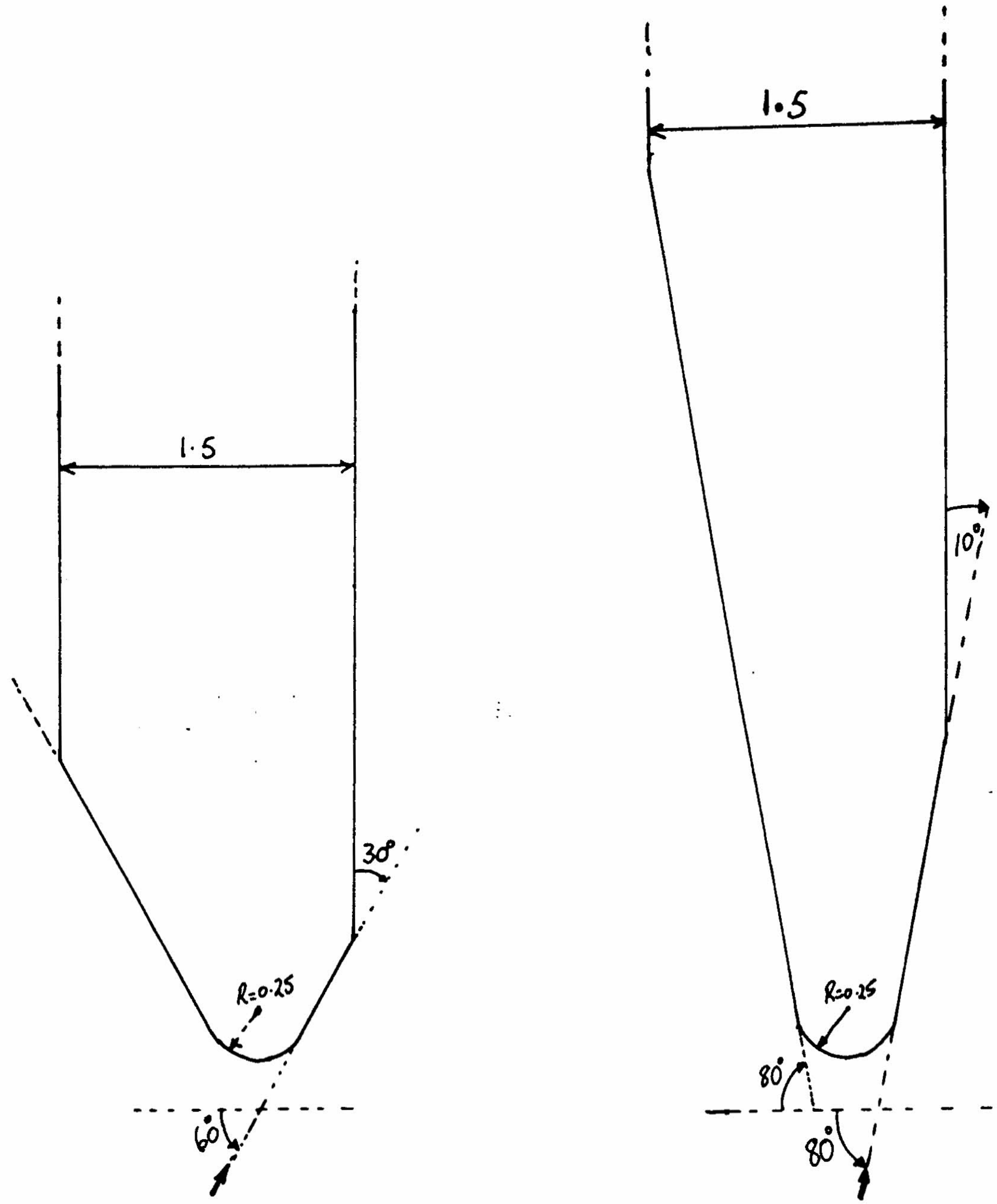

6 (a) 6 (b)

Figure 6.

Alternative designs for telescope-tube front baffle vane-edges used in the GUERAP III model.

Figure 7. Point Source Transmittance (PST)

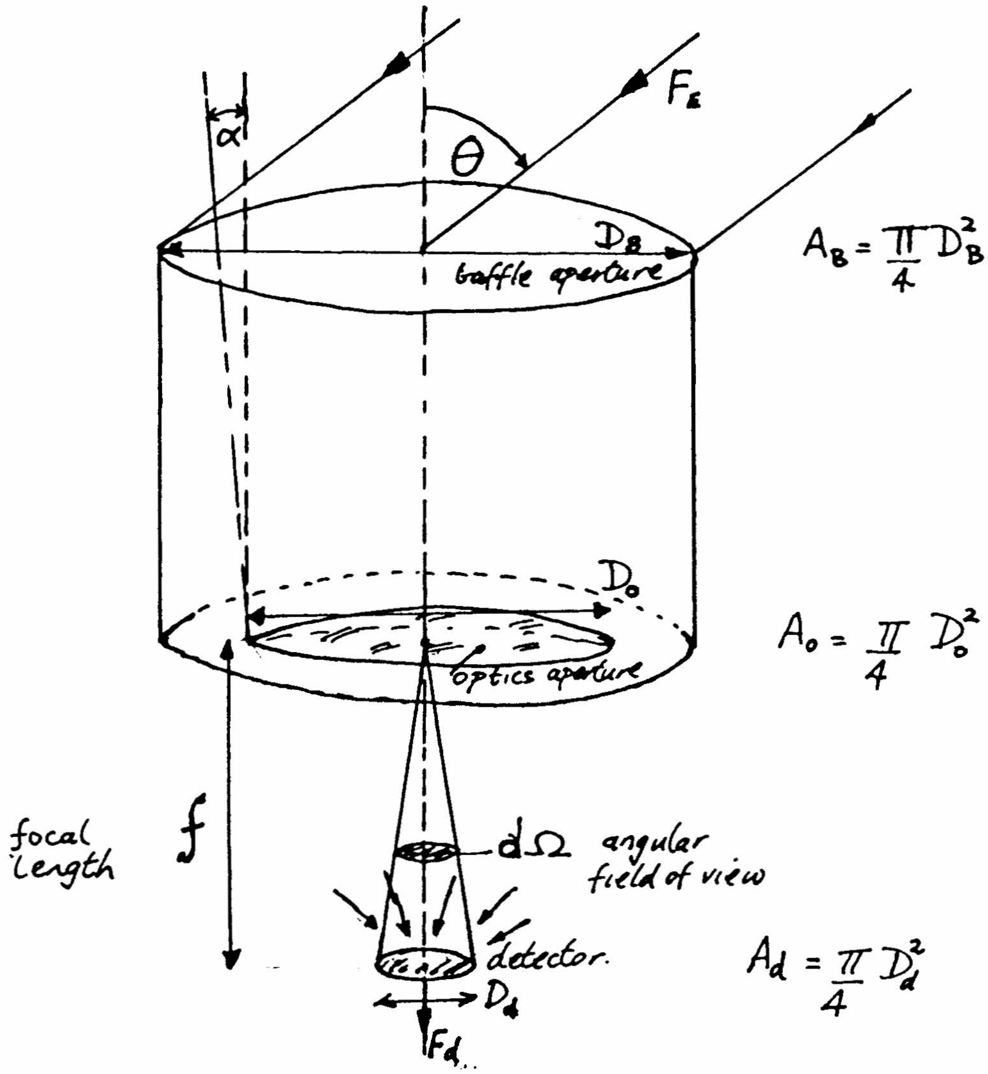

$$PST(\theta) = \frac{F_d}{F_E(\theta)}$$ = POINT SOURCE TRANSMITTANCE AT ANGLE θ° OFF-AXIS OF BAFFLED OPTICAL SYSTEM

F_d = MEASURED OR PERMISSABLE DETECTOR IRRADIANCE (UNITS = ENERGY PER UNIT AREA PER UNIT TIME)

$F_E(\theta)$ = IRRADIANCE AT ENTRANCE APERTURE OF BAFFLE (SAME UNITS AS F_d).

$$a(\theta) = \frac{1}{PST(\theta)}$$ = OFF-AXIS ATTENUATION FACTOR. (COMPUTED BY GUERAP III).

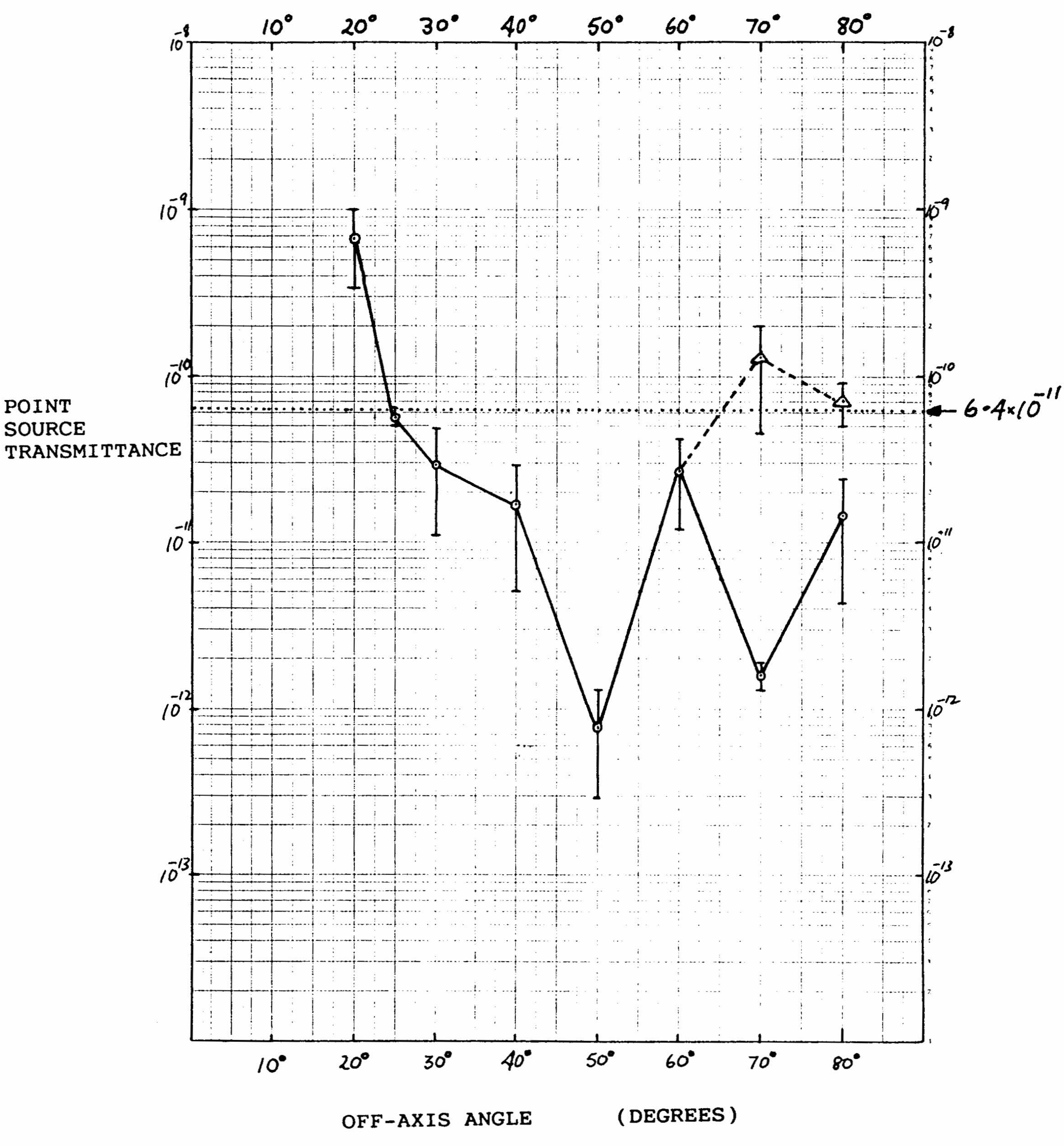

Figure 8. XMM OM Baffle PST v off-axis angle

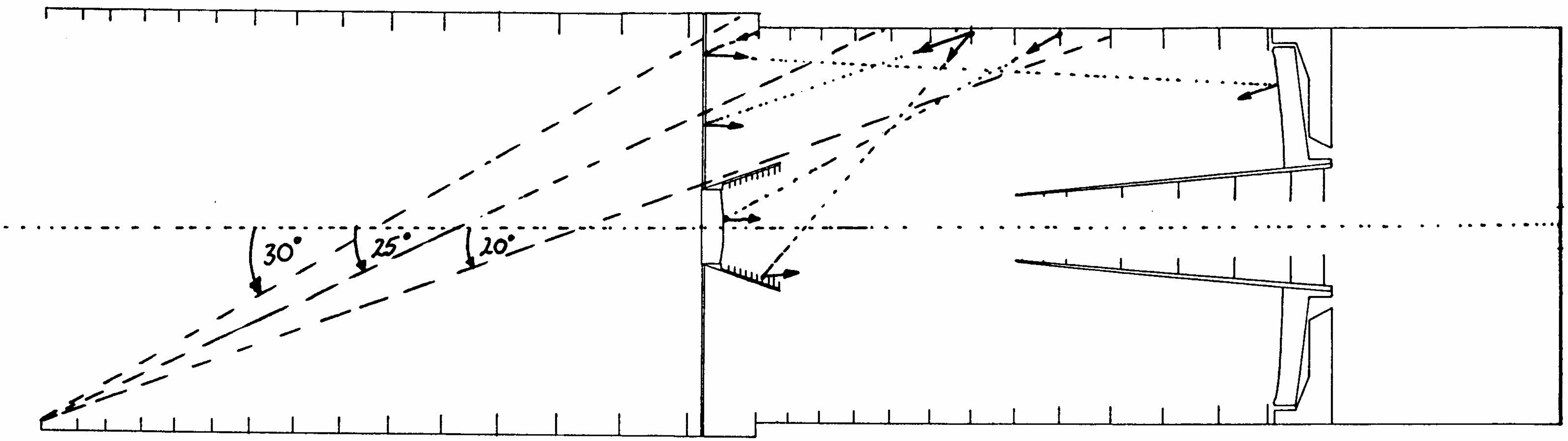

Figure 9. Dominant scattered-light paths for off-axis angles <= 30 degrees

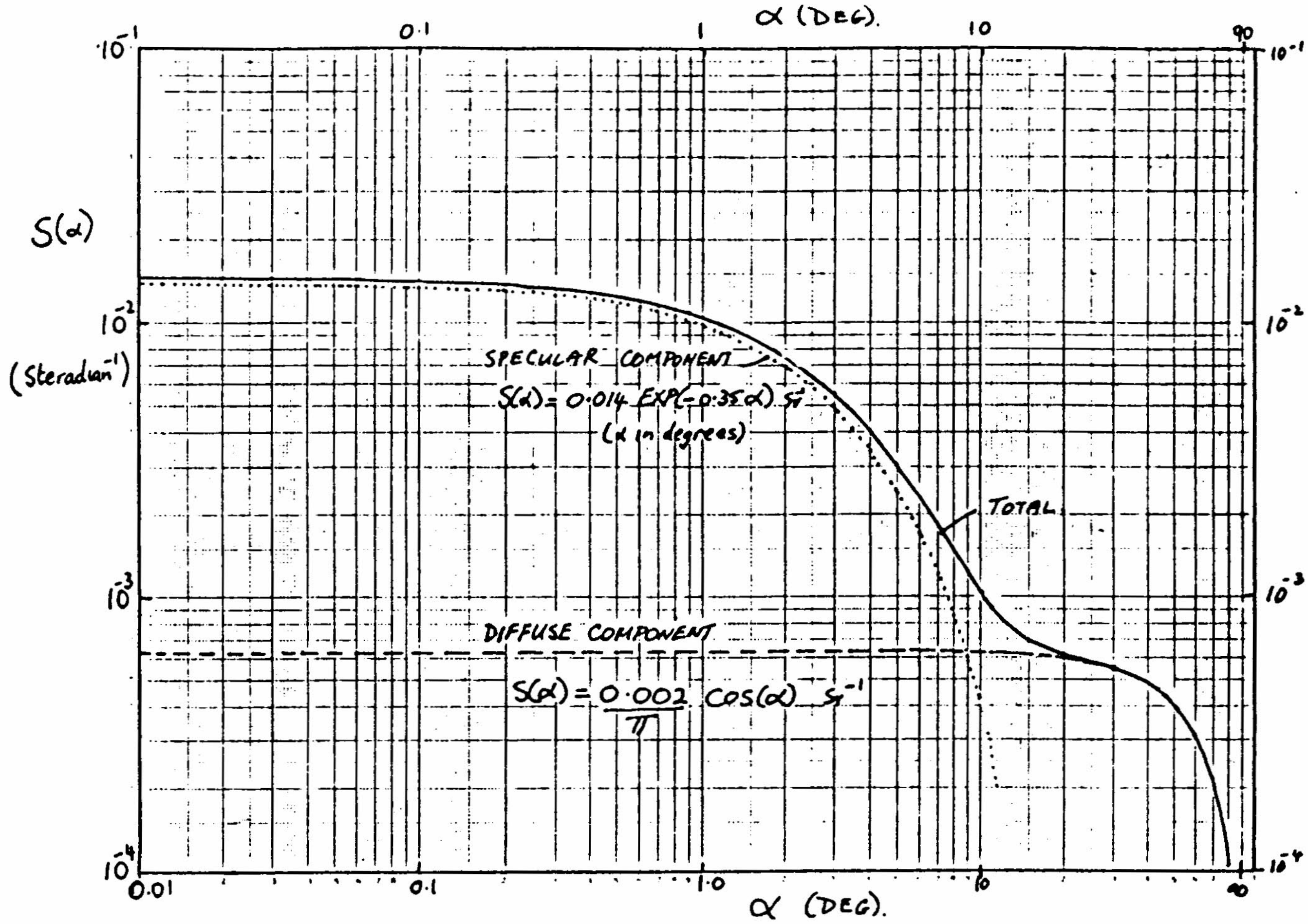

Figure 1a Mirror Scatter Function used in the GUERAP model. α is either the angle from the specular direction (near-specular component) or from the local normal (diffuse component). The curve marked 'Total' will therefore only apply when radiation is incident along a local surface normal. Other 'Total' curves can be generated by shifting the diffuse component horizontally by an an angle equal to the local angle of incidence.

Table 1. Mirror Scatter Functions v Angle

ANGLE (DEG)	SPECULAR SR**-1	DIFFUSE SR**-1	TOTAL SR**-1
0.020	0.139E-01	0.637E-03	0.145E-01
0.030	0.139E-01	0.637E-03	0.145E-01
0.040	0.138E-01	0.637E-03	0.144E-01
0.050	0.138E-01	0.637E-03	0.144E-01
0.060	0.137E-01	0.637E-03	0.143E-01
0.070	0.137E-01	0.637E-03	0.143E-01
0.080	0.136E-01	0.637E-03	0.143E-01
0.090	0.136E-01	0.637E-03	0.142E-01
0.100	0.135E-01	0.637E-03	0.142E-01
0.200	0.131E-01	0.637E-03	0.137E-01
0.300	0.126E-01	0.637E-03	0.132E-01
0.400	0.122E-01	0.637E-03	0.128E-01
0.500	0.118E-01	0.637E-03	0.124E-01
0.600	0.113E-01	0.637E-03	0.120E-01
0.700	0.110E-01	0.637E-03	0.116E-01
0.800	0.106E-01	0.637E-03	0.112E-01
0.900	0.102E-01	0.637E-03	0.109E-01
1.000	0.987E-02	0.637E-03	0.105E-01
2.000	0.695E-02	0.636E-03	0.759E-02
3.000	0.490E-02	0.636E-03	0.553E-02
4.000	0.345E-02	0.635E-03	0.409E-02
5.000	0.243E-02	0.634E-03	0.307E-02
6.000	0.171E-02	0.633E-03	0.235E-02
7.000	0.121E-02	0.632E-03	0.184E-02
8.000	0.851E-03	0.630E-03	0.148E-02
9.000	0.600E-03	0.629E-03	0.123E-02
10.000	0.423E-03	0.627E-03	0.105E-02
20.000	0.128E-04	0.598E-03	0.611E-03
30.000	0.386E-06	0.551E-03	0.552E-03
40.000	0.116E-07	0.488E-03	0.488E-03
50.000	0.352E-09	0.409E-03	0.409E-03
60.000	0.106E-10	0.318E-03	0.318E-03
70.000	0.321E-12	0.218E-03	0.218E-03
80.000	0.968E-14	0.111E-03	0.111E-03
90.000	0.292E-15	0.114E-11	0.114E-11